


Cite this: *RSC Adv.*, 2025, 15, 17476

# Treatment of water discharged from a Yellow River water purification plant: optimization and application of enhanced coagulation technology†

Xiaosan Song,<sup>ID</sup> \*<sup>ab</sup> Hairong Yan,<sup>ab</sup> Qingchao Shen,<sup>\*ab</sup> Wenjing Sun,<sup>ab</sup> Ping Li<sup>ab</sup> and Wenxuan Wei<sup>ab</sup>

In this study, the effects of the coagulant type, compounding ratio, dosage, hydraulic conditions and water temperature on the intensive coagulation process were systematically investigated for the treatment of discharge water with high turbidity and high sediment characteristics from a Yellow River water purification plant (YRWPP). Results indicated that the PFS–PDMDAAC composite coagulant achieved optimal treatment performance under the following conditions: a blending ratio of 6 : 1, a dosage of 13.65 mg L<sup>-1</sup>, rapid mixing at 300 rpm for 1.5 min, slow mixing at 120 rpm for 7 min, and a water temperature of 20 °C. Employing these parameters, supernatant turbidity was reduced to 46.2 NTU, the specific resistance to filtration (SRF) of the sludge was less than 0.94 × 10<sup>12</sup> m kg<sup>-1</sup>, and the solid content exceeded 8%, enabling direct dewatering. With the increase of the concentration of the discharged mud water, the effect of enhanced coagulation is weakened. Specifically, when the concentration was lower than 4.14%, a dosage of 13.65 mg L<sup>-1</sup> could be treated effectively; when the concentration was in the range of 4.14–9.12%, the dosage needed to be increased to 21 mg L<sup>-1</sup>; and when the concentration was more than 9.12%, it was difficult to achieve the discharge standard. Furthermore, zeta potential analysis showed that the absolute zeta potential value was the lowest when the compounding ratio was 6 : 1, and the effect of colloid destabilization was the best. According to floc morphology observation, the volume of floc increased and the structure of floc was loose and porous after enhanced coagulation, which was conducive to settling and dewatering. The analysis of the floc particle size showed that the average floc particle size increased from 38.3 μm to 238 μm at a dosage of 21 mg L<sup>-1</sup>, and the settling performance was significantly improved; when the dosage was more than 21 mg L<sup>-1</sup>, the floc particle size decreased, and the settling performance declined. This study provides technical support for the treatment and resource utilization of mud water discharged from the Yellow River water purification plant.

Received 12th March 2025

Accepted 3rd May 2025

DOI: 10.1039/d5ra01783a

rsc.li/rsc-advances

## 1 Introduction

The Yellow River basin is a typical resource-based water-scarce region in China, with its total water resources accounting for only 2.6% of the country's total water resources and per capita water resources amounting to 1/5 of the national average.<sup>1</sup> In recent years, the decrease in precipitation and the increase in sewage discharge in this basin have led to a decrease in the self-purification capacity of water bodies and an increase in water pollution, where the direct discharge of untreated industrial and domestic sewage is the main source of pollution.<sup>2,3</sup> It is

worth noting that water purification plants, as the core facility for water supply, purify surface water while generating production wastewater, which accounts for 3–8% of the water production volume, mainly consisting of mud drainage water (accounting for 20–50% of the total production wastewater) and other process wastewater. Drainage water mainly from the sedimentation tank mud and filter backwash wastewater, containing high concentrations of suspended solids and organic impurities, if directly discharged will further exacerbate the deterioration of the water environment in the watershed, creating the vicious “pollution–purification–re-pollution” cycle. Discharge mud water is characterized by high turbidity, high sediment content, low organic matter, *etc.*, and its floc particle size is small with a large absolute zeta potential value, which leads to poor dewatering and settling properties. Direct discharge not only pollutes the water environment, but also wastes significant water resources.<sup>4–6</sup> In the context of ecological remediation of the Yellow River basin, the realization of “zero

<sup>a</sup>School of Environmental and Municipal Engineering, Lanzhou Jiaotong University, Lanzhou 730070, China. E-mail: songxs@mail.lzjtu.cn

<sup>b</sup>Key Laboratory of Yellow River Water Environment in Gansu Province, Lanzhou Jiaotong University, No. 88 Anning West Road, Lanzhou 730070, China

† Electronic supplementary information (ESI) available. See DOI: <https://doi.org/10.1039/d5ra01783a>



discharge" and resource utilization of mud drainage water has become an urgent task.<sup>7,8</sup>

At present, the commonly used mud water treatment technology mainly includes natural sedimentation, mechanical dewatering, and chemical conditioning.<sup>9</sup> However, the natural settlement processing efficiency is low, mud–water separation is slow, and it is difficult for the supernatant and precipitated sludge to meet the standard;<sup>10</sup> mechanical dewatering can improve the solid content in sludge, but the processing cost is high, and the effect is limited to high turbidity and high sediment discharge water;<sup>11</sup> chemical conditioning can improve the performance of sludge dewatering,<sup>12</sup> but the treatment effect of a single coagulant is unstable, and it is difficult to cope with the fluctuating water quality of discharge water. Therefore, it is urgent to develop efficient, economical and environmentally friendly mud drainage water treatment technology.<sup>13</sup>

Enhanced coagulation is water treatment technology that improves the removal efficiency of pollutants in water by optimizing the coagulation process. Intensive coagulation, as a highly efficient means of water treatment, has shown significant advantages in mud drainage water treatment in recent years.<sup>14,15</sup> Through the use of composite coagulants,<sup>16</sup> intensive coagulation can not only effectively improve the sedimentation rate and sludge thickening time of sludge water, but also improve the quality of supernatant water, achieving the reuse standard. For example, it has been shown that the polymerized ferric sulfate (PFS) and polydimethyl diallyl ammonium chloride (PDMDAAC) composite coagulant treatment of high turbidity sludge water could significantly improve the floc particle size,<sup>17</sup> improve the settlement performance, and greatly reduce the turbidity of the supernatant to meet the reuse requirements. In addition, enhanced coagulation technology can also enhance the sludge dewatering performance and reduce the subsequent treatment cost through electrical neutralization and adsorption bridging.<sup>18</sup>

This study focused on the treatment of sludge water discharged from the Yellow River water purification plant, aiming to optimize the treatment effect of sludge discharge through enhanced coagulation technology. By systematically studying the effects of the coagulant type, compounding ratio, dosage, hydraulic conditions and other factors on the treatment effect of sludge discharge water, the optimal treatment conditions were determined, and the mechanism of enhanced coagulation was explored. The results of this study can provide technical support for the treatment and resource utilization of mud water from water purification plants, and at the same time lay a theoretical foundation and practical basis for the ecological protection and high-quality development of the Yellow River basin.

## II Materials and methods

### 2.1 Test agent

**2.1.1 Test raw water.** This study employed mud water discharged from a water plant in Lanzhou, Yellow River basin as the object. During the test period, the water quality parameters

of the water purification plant discharge mud water are shown in Table 1.

**2.1.2 Test coagulant.** The coagulants used in this test were all commercial products,<sup>19,20</sup> as follows: polymerized aluminum chloride (PAC) with  $\text{Al}_2\text{O}_3$  mass fraction of 30%, salinity of 70.50%, pH (1% aqueous solution) of 3.5–5.0. Polymeric ferric sulfate (PFS) with full iron content of 22%, salinity of 14%, and pH of 2.0–3.0. Anionic polyacrylamide (APAM) has a molecular weight of 18 million, residual monomer content of 0.021%, hydrolysis degree of 20%, and solid content of 95.1%. Cationic polyacrylamide (CPAM) has a molecular weight of 12 million, ionicity of 30, and solid content of 95.1%. Non-ionic polyacrylamide (NPAM) has a molecular weight of 12 million, a degree of hydrolysis of 10% and a solid content of 95.1%. The viscosity of polydimethyl dipropyl ammonium chloride (PDMDAAC) is 10 000 and the solid content is 40%.

**2.1.3 Other agents required for the test.** The main reagents used in the water quality index testing experiments included: 98%  $\text{H}_2\text{SO}_4$  (analytically pure, Shantou, China),  $\text{Na}_2\text{C}_2\text{O}_4$  (analytically pure, Shanghai, China),  $\text{KMnO}_4$  (analytically pure, Chengdu, China), special reagent for ammonia–nitrogen (SH-NH-100, Jiangsu, China) and total phosphorus (SH-TP-100, Jiangsu, China), platinum and cobalt standard solution (CoPt, analytically pure, Guangzhou, China),  $\text{HNO}_3$  (analytically pure, produced in Tianjin, China), lactose peptone culture solution and EC culture solution (both analytically pure, produced in Guangdong, China).

### 2.2 Test instruments

The key instruments used in the test included TJ6 series program-controlled six coagulation test stirrer produced by Wuhan Hengling Technology Co., Ltd for coagulation stirring; HH-2 digital thermostatic bath produced by Hebei Longshun Instrument Co.; DGG-9070A electric constant temperature blast drying oven for sample drying; Shanghai Xinrui Instrumentation Co., Ltd turbidimeter, used to measure turbidity; Agilent, United States ICP-MS instrument, used to measure the metal content; Nano ZS90 Zeta Potential Tester from Malvern Instruments, UK, to measure the zeta potential; MS 3000 Laser Particle Sizer from Malvern Instruments, UK, to measure the particle size distribution; and JEOL 5600 LV scanning electron microscope from Nippon Electronics Corporation, Japan, to observe floc morphology. These instruments provided the necessary technical support for the smooth running of the experiment.

### 2.3 Testing indicators and methods

**2.3.1 Water quality indicators.** The water quality indicators include turbidity, color, suspended solids (SS), chemical oxygen demand ( $\text{COD}_{\text{Mn}}$ ), ammonia–nitrogen ( $\text{NH}_3\text{-N}$ ), total phosphorus (TP), metal content and microbiological indicators.<sup>21</sup> Turbidity was measured using a turbidimeter,<sup>22</sup> color was measured using the platinum–cobalt standard colorimetric method, suspended solids were measured using the vacuum filtration method, and chemical oxygen demand was measured using the acidic potassium permanganate method.<sup>23</sup> Ammonia–

Table 1 Water quality parameters for mud water discharged from the water purification plant

pH	Solid content	SS	Color	COD <sub>Mn</sub>	NH <sub>3</sub> -N	TP
8.21–8.45	0.4–4.1%	4329–48797		5.04–14.12	36.8–323.6	8.0–78.9
Al	Fe	Mn	Cd	Total bacterial count	Fecal coliform count	
75.1–318.2	10.5–98.1	2.1–9.5	<0.09	6844–53250	3340–24120	

nitrogen was determined by the colorimetric method with nano reagent,<sup>24</sup> total phosphorus was determined by ammonium molybdate spectrophotometry, and metal content was determined by inductively coupled plasma emission spectrometry (ICP-MS).<sup>25</sup> The microbiological indicators include total bacterial count (measured by MPN method) and fecal coliform count (measured by multi-tube fermentation method).<sup>26</sup>

**2.3.2 Sedimentation and dewatering indicators of drainage water.** The indicators of sedimentation and dewatering of drainage water include sedimentation ratio (SV<sub>30</sub>), solid content (*W*) and sludge specific resistance (*r*). The sedimentation ratio is used to measure the sedimentation performance of drainage water, where the smaller the SV<sub>30</sub>, the better the sedimentation performance; the solid rate indicates the concentration of sludge, where the higher the solid rate, the better the dewatering performance; and the specific resistance of sludge reflects its dewatering performance, where the smaller the specific resistance, the better the dewatering performance.<sup>27</sup>

$$SV_{30} = V'/V \times 100\% \quad (1)$$

where *V'* is the volume of sludge settled for 30 min, mL; *V* is the original volume of discharged water, mL.

$$W = (W_3 - W_1)/(W_2 - W_1) \times 100\% \quad (2)$$

where *W* is the solid content, %; *W*<sub>1</sub> is the weight of the evaporation dish, g; *W*<sub>2</sub> is the total weight of the evaporation dish and the sludge discharge water sample, g; and *W*<sub>3</sub> is the total weight of the evaporation dish and the sludge discharge water sample after drying and evaporation, g.

$$r = \frac{2bPA^2}{\mu c} \quad (3)$$

where *r* is the impedance per unit weight, m kg<sup>-1</sup>; *P* is the differential pressure during filtration, Pa; *A* is the filtration area, m<sup>2</sup>; *μ* is the viscosity of the filtrate, Pa s, according to the filtrate temperature lookup table can be obtained from *μ*; *c* is the unit of the filtrate produced by the mud cookies, kg m<sup>3</sup>; and *b* is the slope of the straight line of *t/v-v* measured under a constant vacuum pressure.

**2.3.3 Coagulation mechanism characterization indexes.** The coagulation mechanism characterization indexes include zeta potential, floc morphology and particle size. Zeta potential is used to judge the stability of colloidal particles, where the smaller the absolute zeta potential value, the better the

coagulation effect; floc morphology is observed by scanning electron microscopy; particle size is determined by a laser particle sizer to determine the distribution of the floc particle size.<sup>28</sup>

(1) Zeta potential: this is an important index to characterize the stability of a colloid dispersion system, where its absolute value can directly reflect the settling performance of floc particles in water, enabling the effect of coagulation to be determined. Measurement method: 5 mL of raw water of Yellow River, raw water of drainage water or supernatant after 30 min of coagulation and sedimentation with a syringe at 3 cm below the liquid surface was characterized on a Nano-ZS90 Zeta Potential Tester utilizing the principle of dynamic light scattering.

(2) Floc morphology: the floc morphology during the coagulation process can better reflect the coagulation effect, which is mainly observed through the scanning electron microscopy to determine the morphology of floc particles in the water.

(3) Particle size: the size of the particles in water can reflect the change in floc size during the coagulation process from a microscopic point of view, enabling the coagulation effect to be determined. This test uses a laser particle size meter.

## 2.4 Test steps

The test methods include natural settlement test and enhanced coagulation test. Natural sedimentation test: different concentrations of drainage water were left to settle, the height of the mud-water separation interface was observed, the natural sedimentation curve was plotted, and the quality of the supernatant and sludge indexes was determined. Enhanced coagulation test: the coagulation process was simulated using six stirrers to optimize the coagulation conditions, including the type of coagulant, compounding ratio (1 : 15, 1 : 6, 1 : 3, 1 : 1, 3 : 1, 6 : 1, 15 : 1, 30 : 1, 45 : 1, 60 : 1, and 75 : 1), dosage (5 mg L<sup>-1</sup>, 10 mg L<sup>-1</sup>, 13 mg L<sup>-1</sup>, 15.8 mg L<sup>-1</sup>, 17.8 mg L<sup>-1</sup>, 21 mg L<sup>-1</sup>, 25 mg L<sup>-1</sup>, and 31.5 mg L<sup>-1</sup>), hydraulic conditions (stirring speed and time) and water temperature (5 °C, 10 °C, 15 °C, 20 °C, and 25 °C); the coagulation effect was assessed by determining the turbidity of the supernatant, settling ratio, sludge solid content and specific resistance and other indicators. The specific steps are as follows: (1) selecting the best coagulant type and combination: screening the best combination of coagulants through individual dosing, segmented joint dosing (adapting to changes in water quality and improving the pollutant removal efficiency by phasing in different types of coagulants at different

locations) and compound dosing (combining two or more coagulants (e.g., aluminum salts and polymer flocculants) to improve the coagulation effect); (2) optimizing the compounding ratio: determining the optimal ratio of organic and inorganic coagulants; (3) optimizing the dosage: determining the optimal amount of coagulant; (4) optimizing the hydraulic conditions: determining the optimal mixing speed and mixing time; (5) examining the water temperature: examining the effects of different water temperatures on the coagulation effect; (6) evaluating the coagulation effect through the determination of indicators of supernatant turbidity, sedimentation ratio and specific resistance; and (6) the effect of different concentrations of drainage water and dosages on the coagulation effect: studying the effect of drainage water concentration and dosage on the coagulation effect.

## 2.5 Test methods

### 2.5.1 Optimization of coagulant types and combinations.

To determine the types of coagulants and combinations of coagulants that are most suitable for the treatment of high turbidity and high sediment drainage water from the Yellow River, with the aim of obtaining the optimal combination of composite coagulants, this experiment used two types of inorganic coagulants and four types of organic coagulants for preferential selection. Under room temperature conditions, 1 L of homogeneous muddy water was poured into a 1 L beaker and a six-link stirrer was used to stir it mechanically. Firstly, it was stirred at a speed of 300 rpm for 0.5 min, fully mixing the muddy water in the beaker, and then, a certain amount of PAC, PFS, APAM, CPAM and NPAM was individually added to the beaker quickly, and then stirred at the speed of 300 rpm for 1.5 min, then 300 rpm for 1.5 min, and then a certain amount of PAC, PFS, APAM, CPAM and NPAM quickly added to the beaker. Then, the mixture was stirred for 1.5 min, then slowly at 100 rpm for 5 min, and finally the water samples poured into a cylinder for 30 min to observe and record the mud–water separation interface corresponding to different settling times. Then, the mud–water settling curve was plotted and the settling ratio of  $SV_{30}$ , the turbidity of the supernatant, and preferred coagulant with fast settling speed and low turbidity of the supernatant determined. After optimizing the inorganic and organic coagulants, the same concentration of sludge water was treated with different sequences of section dosing and different combinations of compounding, and the above-mentioned experimental process was repeated to determine the optimal combination of coagulants under a certain amount of coagulant dosage, coagulant compounding ratio and hydraulic conditions.

**2.5.2 Optimization of coagulant mixing ratio.** To determine the optimal ratio of organic and inorganic coagulants in the best composite coagulant, the optimal coagulant mixing ratio was determined, thus improving the coagulation efficiency. In this test, different mixing ratios were used at room temperature, where the mud drainage water was first stirred to homogeneity (300 rpm stirring for 0.5 min), and then the same coagulant dosage was subjected to a fast stirring stage (300 rpm

fast stirring for 1.5 min), slow flocculation stage (100 rpm slow stirring for 5 min), left to stand for 30 min at the end of the slow flocculation stage, and the turbidity of the supernatant measured and the mud–water separation interface observed at different intervals. The coagulation evaluation indexes were  $SV_{30}$  and supernatant turbidity, optimizing the mixing ratio.

**2.5.3 Optimization of coagulant dosage.** After determining the optimal compound coagulant and compounding ratio, a variety of coagulant dosages was used to treat the sludge discharge water, and the coagulation and mixing process was repeated under unchanged room temperature and hydraulic conditions, and the dosage was optimized using the settling ratio of  $SV_{30}$  and the supernatant turbidity as the coagulation evaluation indexes.

**2.5.4 Optimization of hydraulic conditions.** The coagulation process mainly controls the hydraulic conditions through two stages, the fast stirring stage and the slow flocculation stage, and the stirring speed and stirring time of different stages represent different hydraulic conditions. Therefore, under room temperature conditions, this experiment optimized the hydraulic parameters of stirring speed and stirring time of the two phases, and the best hydraulic conditions were determined using the settling ratio  $SV_{30}$  and supernatant turbidity as the coagulation evaluation indexes. For the optimization of the stirring speed parameter, the stirring time of the two stages was fixed as follows: fast stirring time was 1.5 min, slow stirring time was 5 min, thus optimizing the stirring speed of the different stages; for the optimization of the stirring time parameter, the stirring time of the two stages was fixed as follows: the optimal fast stirring speed and slow stirring speed, thus optimizing the stirring time of the different stages.

**2.5.5 Examination of water temperature.** Drainage water was placed in an incubator, and the water temperature was incubated to 5 °C, 10 °C, 15 °C, 20 °C and 25 °C, respectively. The preferred composite coagulant was used to carry out intensive coagulation tests on drainage water with different temperatures under the optimal dosage and hydraulic conditions. The coagulation operation remained unchanged, and the optimum water temperature for the enhanced coagulation of drainage water was selected using the sedimentation ratio  $SV_{30}$  and supernatant turbidity as the evaluation indexes of coagulation.

**2.5.6 Examination of the coagulation effect of different concentrations of drainage water and coagulant dosages.** Adopting the optimal parameters of intensive coagulation and employing the sedimentation ratio  $SV_{30}$  and turbidity of the supernatant as the evaluation indexes of the coagulation effect, intensive coagulation tests were carried out on the discharged sludge with different solid contents, and intensive coagulation tests were also carried out on the highly concentrated discharged sludge using different dosages to investigate the effects of the concentration of discharged sludge and the dosage of coagulant on the coagulation effect. Under different working conditions, the specific resistance of sludge and solid content were measured to evaluate the dewatering performance, and the turbidity, color, pH, potassium permanganate index, ammonia–nitrogen, total phosphorus, dissolved metals, microorganisms



**Table 2** Water quality parameters of supernatant after natural sedimentation of different concentrations of drainage water<sup>a</sup>

pH	Turbidity	Color	COD <sub>Mn</sub>	NH <sub>3</sub> -N	TP
8.2–8.5	80.1–791.5	13–29	2.65–3.65	0.65–18.5	0.11–1.25
Al	Fe	Mn	Cd	Total bacterial count	Fecal coliform count
0.62–2.8	0.3–1.5	0.08–0.67	<0.004	3550–8600	1550–4050

<sup>a</sup> The units of water quality indicators are as follows: CFU mL<sup>-1</sup> for total bacteria; mpn per mL for fecal coliform; SS, COD<sub>Mn</sub>, NH<sub>3</sub>-N, TP and other water quality indicators are in mg L<sup>-1</sup>.

and acrylamide monomer content of the supernatant were measured to evaluate the safety of the water quality.

## 2.6 Data processing and analysis

The enhanced coagulation performance was evaluated by plotting sedimentation curves, measuring water quality parameters, and analyzing the floc morphology and particle size distribution, with further discussion on the coagulation mechanisms involved (Table 2).

# 3 Results and discussion

## 3.1 Settling performance of different concentrations of discharge water

Before carrying out the enhanced coagulation test, it was necessary to carry out a natural settlement test to investigate the natural settlement performance of different concentrations of drainage water, as well as the quality of the supernatant, the solid content in the sludge at the bottom and the specific resistance of the sludge after 30 minutes of settlement. The specific test method is as follows: the test device was a glass cylinder with a diameter of 67 mm and height of 415 mm, with a scale on the cylinder. After mixing different concentrations of sludge water, 1000 mL of sludge water was placed in a 1 L glass cylinder for settling. The height of the mud–water separation interface at each settling time point was observed and recorded, and the natural settling curve of different concentrations of drainage water drawn; after mixing different concentrations of drainage water evenly and pouring it back into the 1 L glass measuring cylinder for 30 min, a certain amount of supernatant was taken out from the drainage water and the bottom sludge with a syringe and catheter to measure the water quality, solid content and the specific sludge resistance, respectively.

During the test, it was found that when the sludge concentration was too low, the sludge settling process did not have obvious settled layer and a very clear mud–water separation interface was not formed, and thus it could not be observed accurately. After completion of the test, a series of test data on the height of the mud–water separation interface with different settling times was obtained, which was employed to plot the natural settling curves of different concentrations of discharged

sludge water, and the concentration of discharged sludge water was expressed in terms of solid content (%), as shown in Fig. 1. As can be seen in Fig. 1, in the natural sedimentation of drainage water, the sedimentation velocity decreased with an increase in time, and the higher the concentration, the slower the sedimentation, the poorer the sedimentation and the smaller the concentration factor. When the concentration was less than 0.834%, the settling speed was fast, the pressure point was reached within 10 min, the height of the mud–water separation line was basically unchanged after settling for 30 min, and the SV<sub>30</sub> reached 5%; when the concentration was higher than 1.41%, the mud–water separation line slowed down, and the time curve tended to be flat, and the pressure point was not obvious, for example, the SV<sub>30</sub> of the drainage water with 4.23% and 9.12% solid content was as high as 40.5% and 67.5%, respectively, after natural settling, and the concentration multiplier was small. This may be due to the fact that with an increase in concentration, the number of colloidal particles increase, the spacing becomes smaller, the particles are disturbed by the settlement, and the interaction force and resistance increase, limiting rapid settlement. Therefore, the natural sedimentation rate of the high-concentration drainage water was slow, with a poor performance and low concentration, which is unfavorable for treatment.

After examining the settling performance, the supernatant and bottom sludge of the discharged water after 30 min of natural settling were tested for the relevant indexes. The results showed that natural sedimentation could remove a large amount of suspended solids, and the content of suspended solids, COD, NH<sub>3</sub>-N, TP, metals and microorganisms in the supernatant was greatly reduced; however, compared with the source water quality of the Yellow River (see Table S1 in the ESI†) and the effluent standards (turbidity < 50 NTU) of Water Plant No. 1, the supernatant of the sludge dewatering effluent still exhibited higher turbidity and other elevated indicators. Direct reuse may disrupt water treatment processes and pose potential water quality safety risks. As shown in Table 3, from the perspective of sludge characteristics, the solid content of the sedimented sludge from sludge dewatering effluent at different

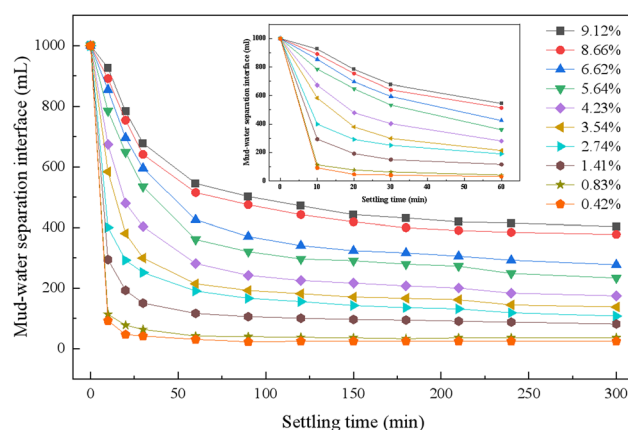


**Fig. 1** Natural settling curves for different concentrations of drainage water.

**Table 3** Indicators of sludge after natural settling of different concentrations of discharged water

Solid content	Sludge specific resistance ( $10^{12} \text{ m kg}^{-1}$ )
6.7–14.5	6.2–12.8

concentrations exceeded 6%, and the specific resistance to filtration (SRF) was greater than  $6.2 \times 10^{12} \text{ m kg}^{-1}$ . Generally, sludge with an SRF of  $>1.0 \times 10^{10} \text{ m kg}^{-1}$  is classified as difficult-to-filter sludge, while sludge with an SRF in the range of  $0.5\text{--}0.9 \times 10^{12} \text{ m kg}^{-1}$  is considered moderately filterable, and sludge with an SRF of  $<0.5 \times 10^{12} \text{ m kg}^{-1}$  is deemed easy to filter. The naturally settled sludge in this study falls in the category of high-concentration, difficult-to-filter sludge. Although its solid content meets the feed requirements for dewatering equipment, its excessively high SRF and poor dewaterability make it unsuitable for efficient dewatering processes.

### 3.2 Research on the influencing factors of intensive coagulation treatment of drainage water

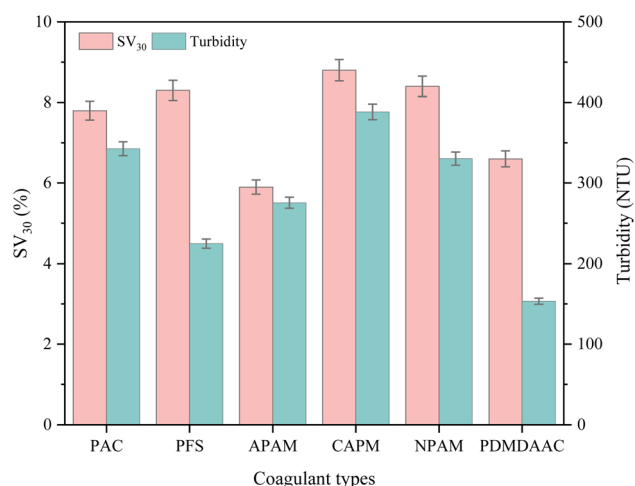
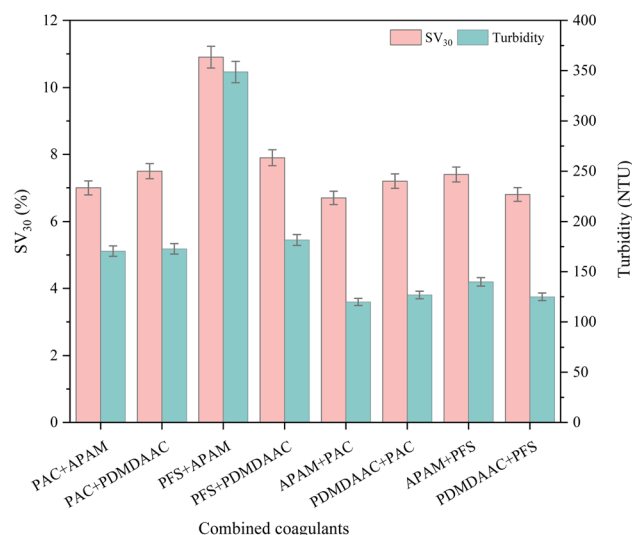
**3.2.1 Influence of coagulant type and dosing order on the coagulation effect.** In the test of enhanced coagulation of discharged water, a six-link stirrer was used to simulate the coagulation process of water purification plant, and the influencing factors were optimized to improve the settling performance, concentration ratio and effluent quality of discharged water with high turbidity and high sediment. Fig. 2 shows the effect of different coagulants on the effectiveness of the drainage water. The results showed that among the organic coagulants, APAM had strong adsorption and bridging effects due to its large molecular weight and long chain length, and could form flocs with rapid stirring and had an excellent settling performance. PDMDAAC formed dense flocs through electrical neutralization and adsorption bridging, and had significant flocculation and turbidity removal ability. In contrast, CPAM and NPAM had

a poor coagulation effect due to their low molecular weight, short chains and weak adsorption bridging effect. Among the inorganic coagulants, although PAC flocs were formed earlier, their density was low and they were easy to break, resulting in higher turbidity of the supernatant; PFS flocs were formed later, but formed high-density flocs, with stronger turbidity removal ability.<sup>29</sup>

In the segmental coagulation test, it can be seen in Fig. 3 that the effect of different coagulant combinations on the sedimentation ratio and turbidity varied significantly. The “PFS + PDMDAAC” combination had the highest settling ratio of 10.9% and turbidity of 348.7 NTU, indicating that the sludge settling performance was poor and the water was turbid. The combination of “APAM + PAC” had the lowest turbidity of 119.8 NTU, and the combination of “APAM + PFS” had the lowest settling ratio of 6.7%, which showed that these two combinations performed better in reducing the turbidity and improving the settling performance.

This result originated from the coagulant mechanism and synergistic effect. Different coagulants have different compositions, structures, adsorption of suspended particles, bridging and electrical neutralization ability.<sup>30</sup> Part of the combination can effectively neutralize the charge to promote the aggregation of particles to reduce the turbidity and accelerate the settlement; part of the combination has poor interaction, making the particles difficult to aggregate and settle, and thus the settling ratio and turbidity are high.

In the single dosage compound coagulant test, the dosage of inorganic coagulants PAC and PFS was  $9 \text{ mg L}^{-1}$ , and the dosage of organic coagulants APAM and PDMDAAC was  $1.5 \text{ mg L}^{-1}$ . The inorganic coagulants and organic coagulants were compounded into a compound coagulant according to the ratio of 6 : 1, and then dosed in the rapid stage, where “PAC–APAM” indicates that PAC and APAM were compounded and added in the rapid mixing stage, and the others

**Fig. 2** Effect of different coagulants on the coagulation effect of drainage water.**Fig. 3** Effect of different coagulant combinations and dosing order on the coagulation effect.

are similar, and the coagulation effect after 30 min of static sedimentation is shown in Fig. 4. Fig. 4 shows that the “PFS–APAM” combination had the highest settling ratio of 10.7%, turbidity of 305.6 NTU, poor sludge settlement and turbid water; the “PFS–PDMDAAC” combination was the best, with a settling ratio as low as 5.1%, turbidity of 88.0 NTU, and the effect of sedimentation and turbidity reduction was significant. The difference is due to their different coagulant characteristics and synergistic effect. “PFS–PDMDAAC” showed good electric neutralization, adsorption and bridging and promoted particle settlement; ‘PFS–APAM’ interaction was not conducive to particle aggregation, resulting in poor sedimentation and turbidity control. Therefore, PFS–PDMDAAC was chosen to treat the high turbidity and high sediment discharge water from the Yellow River in this experiment, which is expected to be highly efficient and ensure that the water quality meets the standard, providing reliable support for the water treatment project.

**3.2.2 Influence of coagulant compounding ratio on coagulation effect.** The optimal compounding ratio of the PFS–PDMDAAC composite coagulant was investigated to achieve an enhanced coagulation performance in treating sludge water from a Yellow River source water treatment plant. In this experiment, sludge water with a solid content of 1.5% was utilized, with a coagulant dosage of  $10.5 \text{ mg L}^{-1}$ , while maintaining consistent coagulation and hydraulic parameters. Specifically, 1 L of sludge water was poured into a 1 L beaker and mixed uniformly at a stirring speed of 300 rpm for 0.5 min. During the rapid mixing phase, different compounding ratios of the PFS–PDMDAAC composite coagulant were added. The rapid mixing and slow flocculation phases were conducted at 300 rpm for 1.5 min and 100 rpm for 5 min, respectively. Subsequently, the mixture was transferred to a measuring cylinder and allowed to settle for 30 min. The sludge volume index ( $\text{SV}_{30}$ ) and supernatant turbidity were measured to determine the optimal compounding ratio of the PFS–PDMDAAC composite coagulant (defined as the ratio of PFS dosage to PDMDAAC dosage, *i.e.*, PFS dosage : PDMDAAC dosage). The test results are illustrated in Fig. 5.

According to the test results, the coagulation effect showed regular changes with the compounding ratio under the same concentration of discharge water, dosage of coagulant and other coagulation conditions. When the compounding ratio was 6 : 1, the coagulation effect was the best, the turbidity of the supernatant was only 79.6 NTU, and the  $\text{SV}_{30}$  was 5.1%. The coagulation effect was the worst when the ratio was 1 : 15. In the process of changing the mixing ratio, too much or too little organic coagulant content led to a poor coagulation effect, where only 6 : 1 formed the ideal high-density floc to achieve rapid settlement.

**3.2.3 Influence of coagulant dosage on coagulation effect.** Under the same hydraulic conditions at room temperature, different dosages of PFS–PDMDAAC composite coagulant with a mixing ratio of 6 : 1 were used to strengthen the coagulation test, and the effects of different dosages on the coagulation effect are shown in Fig. 6. The test results showed that the coagulant dosage was positively correlated with the enhanced coagulation effect. When the dosage was in the range of  $5.25$  to  $13.5 \text{ mg L}^{-1}$ , the turbidity of the supernatant and the sedimentation ratio of  $\text{SV}_{30}$  decreased significantly, and the coagulation effect was enhanced. This is mainly due to the increase in the number of positively charged groups and polymer chains, which enhanced the electrical neutralization and adsorption bridging effect, and facilitated the aggregation of colloidal particles to form larger flocs. When the dosage was increased from  $13.5 \text{ mg L}^{-1}$  to  $21 \text{ mg L}^{-1}$ , the enhancement in coagulation effect slowed down; when the dosage was increased to  $31.5 \text{ mg L}^{-1}$ , the turbidity of the supernatant slowly increased, the  $\text{SV}_{30}$  increased, and the effect deteriorated, which may be due to the restabilization of the colloid and the colloidal protective effect of the polymer chains caused by the over-dosage. When the dosage was  $13.65 \text{ mg L}^{-1}$ , the turbidity of the effluent was 46.2 NTU, which meets the requirements of the effluent of a water plant and can be reused. A further increase in the dosage had limited effect, and thus may lead to the waste of

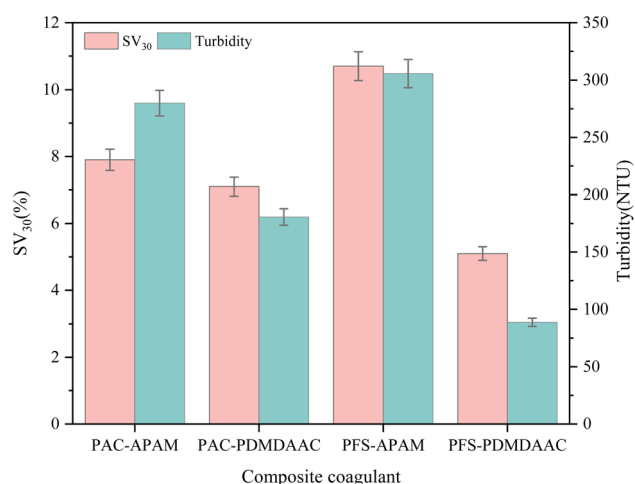


Fig. 4 Effect of different composite coagulant combinations on the coagulation effect.

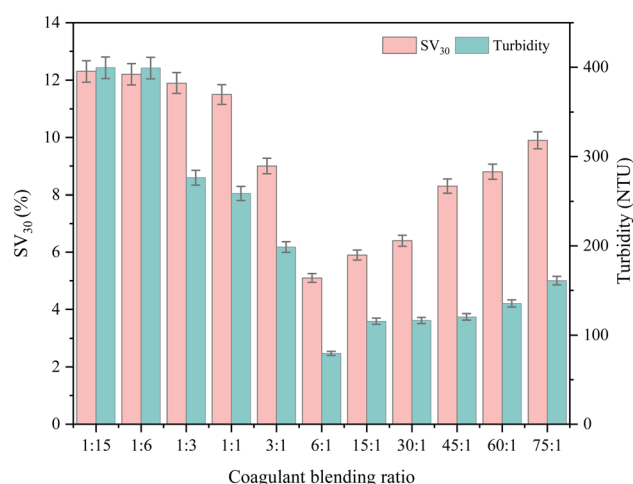


Fig. 5 Impact of different PFS–PDMDAAC composite coagulant ratios on coagulation performance.

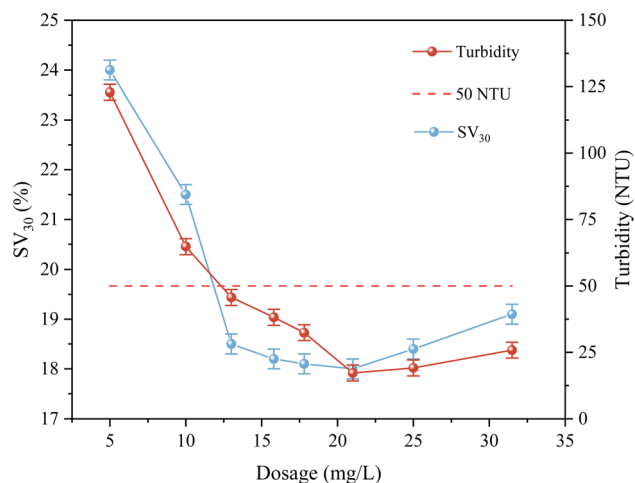


Fig. 6 Impact of different dosages of PFS-PDMAAC composite coagulants on coagulation performance.

chemicals and increase in the content of organic matter in the effluent (Table 4).

**3.2.4 Influence of hydraulic conditions on coagulation effect.** In the process of coagulation treatment, from the perspective of coagulation kinetics, it is significant to determine the optimal hydraulic conditions to strengthen the coagulation effect. The coagulation process consists of three stages including rapid mixing, slow flocculation and static precipitation. In this test, the PFS-PDMAAC composite coagulant was employed with the compounding ratio of 6 : 1, and under the conditions of specific dosage and discharge water, the influence of mixing speed and mixing time on the effect of coagulation was investigated in the different stages.

(1) *Effect of stirring speed on coagulation effect.* Fig. 7 shows the effect of stirring speed on  $SV_{30}$  and turbidity. With an increase in the stirring speed,  $SV_{30}$  and turbidity showed fluctuating changes. At a lower stirring speed,  $SV_{30}$  and turbidity were higher, indicating poorer settling and coagulation effects; thus, an appropriate increase in stirring speed can significantly improve the settling performance and reduce the turbidity. However, a too high stirring speed may lead to floc fragmentation, causing  $SV_{30}$  and turbidity to increase again and affecting the coagulation effect. Therefore, a moderate stirring speed (e.g., 300 rpm) is the most conducive to optimizing the coagulation effect.

In addition, the stirring speed in the rapid mixing stage had a greater influence on the coagulation effect. On the one hand,

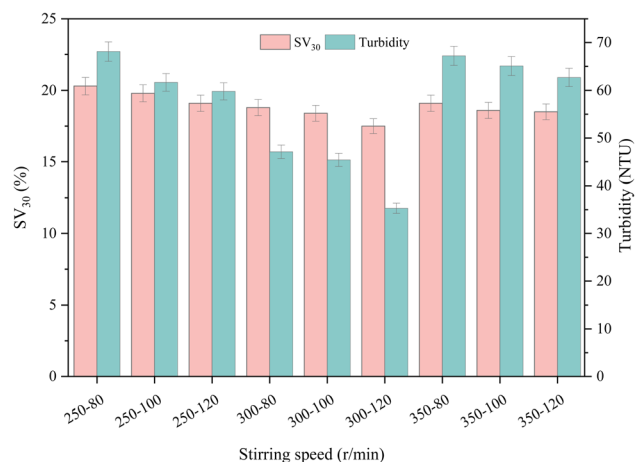


Fig. 7 Effect of different mixing speeds on the coagulation effect.

this is because of the polymer chains in PFS-PDMAAC in this stage and colloid particle adsorption bridging effect at the same time, where the high-density positively charged groups and the negatively charged colloids in the water have strong adsorption neutralization; on the other hand, there is a problem of homogeneous mixing of the polymer chains in the rapid stirring stage, and the degree of adsorption bridging effect in slow flocculation stage is dependent on the degree of flocculation destabilization and cohesion in the rapid stage.

(2) *Influence of stirring time on the coagulation effect.* The optimal mixing speed was 300 rpm for fast mixing and 120 rpm for slow mixing to study the effect of different mixing times on the coagulation effect, and the test results are shown in Fig. 8. As can be seen in this figure, the optimal time for the fast mixing stage is 1.5–7 min. Too short a time (1–1.5 min) will lead to uneven mixing of the PFS-PDMAAC polymer chains, which will affect the destabilization and settlement of the flocs; too long a time (1.5–2 min) will destroy the flocs due to the strong shear force, which will increase the turbidity of the effluent.

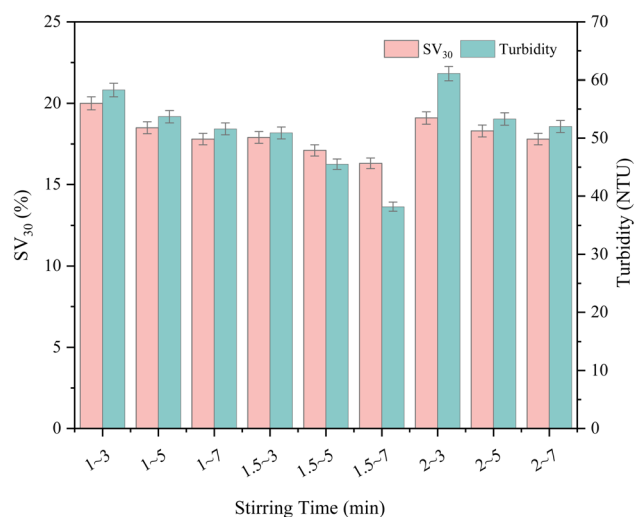


Fig. 8 Effect of different mixing times on the coagulation effect.

Table 4 Particle size of drainage water with different dosages

Experimental protocol	$D_{10}$	$D_{50}$	$D_{90}$	Average particle size
Raw drainage water	28.3	39.7	54.6	38.3
Dosage 5.25 mg L <sup>-1</sup>	53.6	91.1	152	84
Dosage 21 mg L <sup>-1</sup>	181	244	328	238
Dosage 31.5 mg L <sup>-1</sup>	66.7	107	173	101



Thus, the best time for the slow flocculation stage is 7 min, where prolonging the mixing time can promote the polymer chain adsorption bridging colloidal particles, forming dense flocs and improving the coagulation effect. The rapid mixing stage has a more significant effect on the coagulation effect. Therefore, the optimal hydraulic conditions were 300 rpm for 1.5 min for fast mixing and 120 rpm for 7 min for slow mixing. This condition can significantly improve the coagulation effect, provide important technical parameters for the water treatment process, ensure that the water quality meets the standard and improve the treatment efficiency.

### 3.2.5 Influence of water temperature on coagulation effect.

The sludge discharge from the Yellow River basin water purification plant in the summer period is characterized by high concentration, where the water temperature changes day and night, and thus water temperature has a significant impact on the coagulation effect. The sedimentation curves of the discharged mud water with different water temperatures and the effect on the coagulation effect are shown in Fig. 9. During natural sedimentation, the sludge interface decreased slowly at 5 °C, and the suspended particles were in a gelatinous state; with the increase in the water temperature, the sedimentation speed was accelerated, and the best effect was achieved at 20 °C. After intensive coagulation, when the water temperature was

increased from 5 °C to 20 °C, the turbidity of the supernatant decreased from 52.5 NTU to 35.6 NTU, and the  $SV_{30}$  decreased from 17.1% to 15.5%; and when the water temperature increased from 20 °C to 25 °C, the turbidity of the supernatant increased back to 45.05 NTU and the  $SV_{30}$  increased to 16.6%. At 5 °C, the coagulation effect was poor because the low temperature increased the viscosity, weakened the Brownian motion of the colloidal particles, and the floc formation was slow and loose; at 25 °C, the effect was reduced, probably because the high temperature caused the aging and decomposition of the organic polymer flocculant; the best enhanced coagulation effect at 20 °C was attributed to the fact that PFS maintained efficient flocculation at low temperatures, generated more alum flowers, and the polymer chain of PDMDAAC had a good effect on colloid bridging. Generally, the sedimentation and turbidity of the effluent after intensive coagulation were good, and basically meet the water quality requirements.

### 3.3 Research on influencing factors of supernatant water quality and sludge settleability of drainage water

To improve the treatment effect of high turbidity and high sediment discharge water, it is necessary to optimize the sludge settling, concentration ratio and effluent water quality to ensure the safety of reuse. The concentration of discharge water

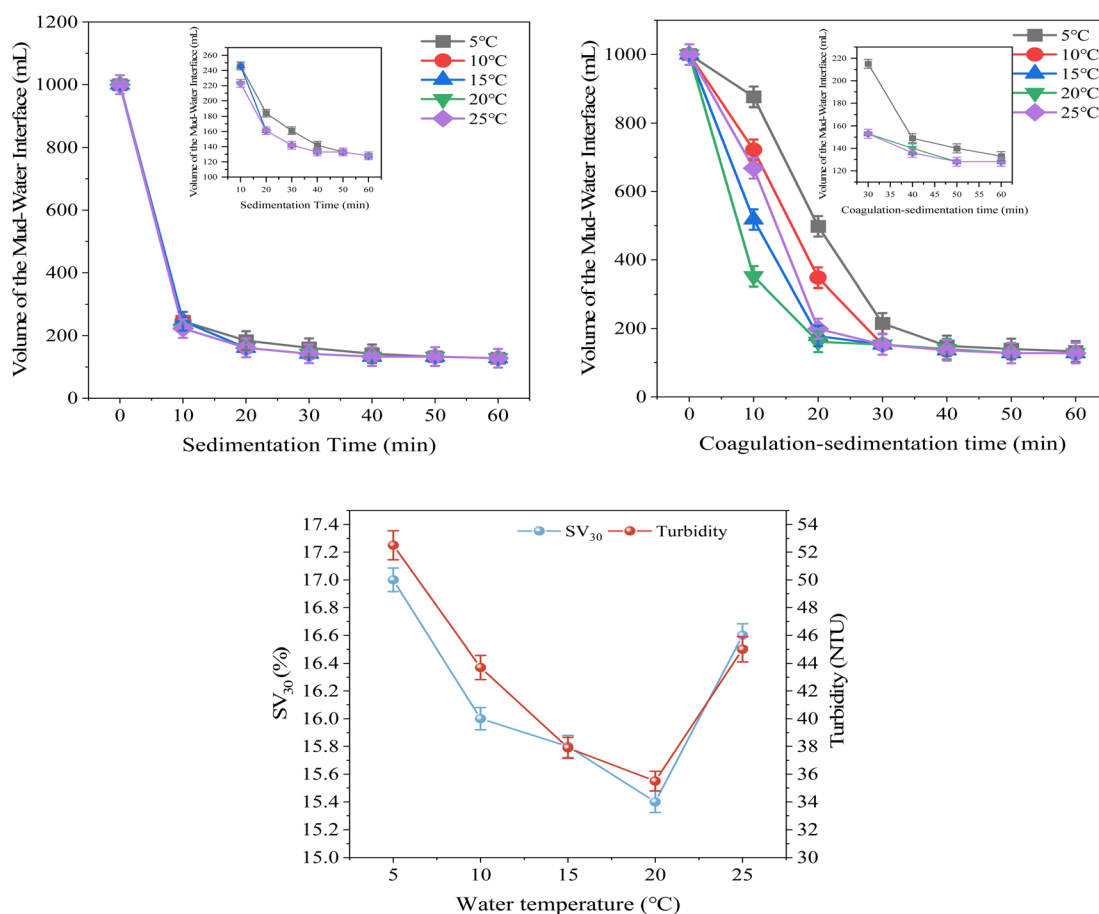


Fig. 9 Settling curves of drainage water with different water temperatures and the effect on the coagulation effect.

fluctuates significantly during the abundant water period, and the content of pollutants increases with the concentration, which directly affects the concentration ratio of coagulated sludge and the quality of supernatant (e.g., turbidity,  $\text{COD}_{\text{Mn}}$ ,  $\text{NH}_3\text{-N}$ , TP, metals and microorganisms). In this case, it is difficult for a fixed coagulant dosage to guarantee sludge settleability and effluent water quality safety. Therefore, the concentration of the discharge water and coagulant dosage were used as variables to investigate their effects on the sludge settlement ratio ( $\text{SV}_{30}$ ) and supernatant water quality indexes under the optimal conditions of enhanced coagulation, achieving the efficient and safe reuse of the supernatant and reducing the amount of subsequent sludge treatment.

**3.3.1 Influence of sludge concentration and dosage on sludge settleability after coagulation.** Fig. 10 indicates that at the same coagulant dosage, a higher concentration of sludge water results in a larger settled sludge volume ( $\text{SV}_{30}$ ) after enhanced coagulation, indicating a poorer sludge settling performance.

In the concentration range of 0.608–1.84%, increasing the dosage only led to a slow rise in  $\text{SV}_{30}$ , with no significant improvement in settling performance. Excessive dosing may even reduce the settling velocity. For concentrations in the range of 1.84–4.14%,  $\text{SV}_{30}$  initially decreased, and then increased, showing a limited enhancement in settling performance, while overdosing had a negative impact.

In the range of 4.14–9.12%, increasing the dosage significantly improved the settling performance, with  $21 \text{ mg L}^{-1}$  being the optimal dosage. However, excessive dosing led to a deterioration in performance. When the concentration was below 4.14%, the optimal dosage was  $13.65 \text{ mg L}^{-1}$ . In the concentration range of 4.14–9.12%, the dosage could be gradually increased to  $21 \text{ mg L}^{-1}$  to optimize the settling performance.

As shown in Table S2,<sup>†</sup> the solid content of the coagulated sludge fluctuated between 8.04% and 22.37%, which could

meet the sludge feeding requirements of various types of dewatering equipment; the specific resistance of the sludge was in the range of  $0.15\text{--}1.04 \times 10^{12} \text{ m kg}^{-1}$ , which belonged to the sludge with easy filtration or moderately easy filtration. Due to the high solid rate and small specific sludge resistance of the sludge treated under the best enhanced coagulation conditions, the sludge dewatering performance was good, which would greatly reduce the difficulty of sludge dewatering in the water purification plant and enables the water purification plant to choose more suitable dewatering equipment according to its own needs. In the case of the sludge with 9% solid content, it was only necessary to increase a certain amount of coagulant to improve the settling speed of the sludge, reduce the specific sludge resistance and improve the dewatering performance, meeting the requirements of sludge dewatering in water purification plants.

**3.3.2 Influence of concentration and dosage of discharged mud water on supernatant water quality.** The influence of the concentration of mud drainage water and coagulant dosage on the supernatant water quality was investigated with reference to a water plant effluent water quality or other reuse standards.

Regarding the concentration of discharge water, as shown in Fig. S1 and S2 in the Appendix,<sup>†</sup> under the optimal conditions of intensive coagulation, with an increase in concentration, the indicators of the supernatant increased and the water quality became worse. When the concentration was less than 4.14%, the turbidity of the supernatant was less than 50 NTU and most of the indicators met the standard; when the concentration increased from 4.14% to 9.12%, the turbidity and other indicators significantly increased. In terms of specific indicators, as shown in Fig. 11 and 12, an increase in concentration increased the turbidity and color, but at high concentrations, PFS-PDMAAC still had strong ability to remove turbidity and color. In the case of  $\text{COD}_{\text{Mn}}$ ,  $\text{NH}_3\text{-N}$  and TP, an increase in concentration led to an increase in their content, although some of the indicators still met the relevant standards after the coagulation of high-concentration drainage water. The metal and microbial

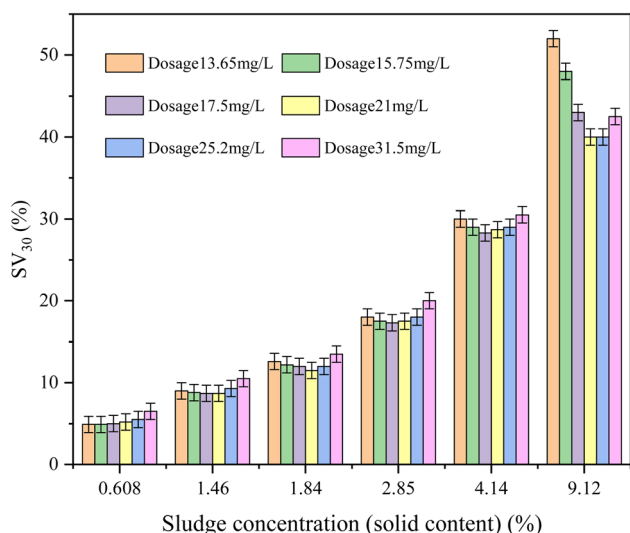


Fig. 10 Effect of discharge water concentration and dosage on sludge settleability after coagulation.

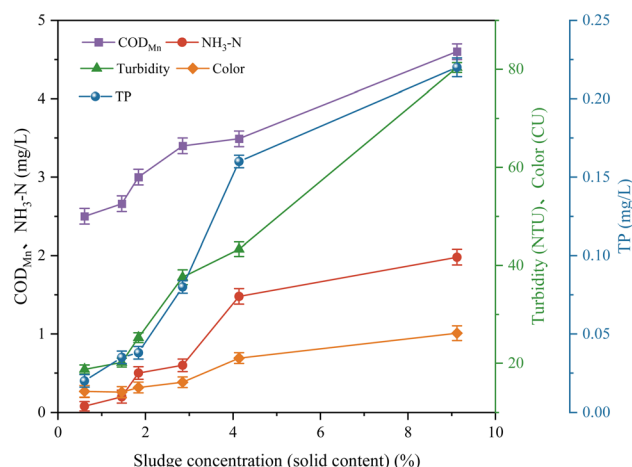


Fig. 11 Effect of discharge water concentration on  $\text{COD}_{\text{Mn}}$ ,  $\text{NH}_3\text{-N}$ , TP, turbidity and color of supernatant liquid.

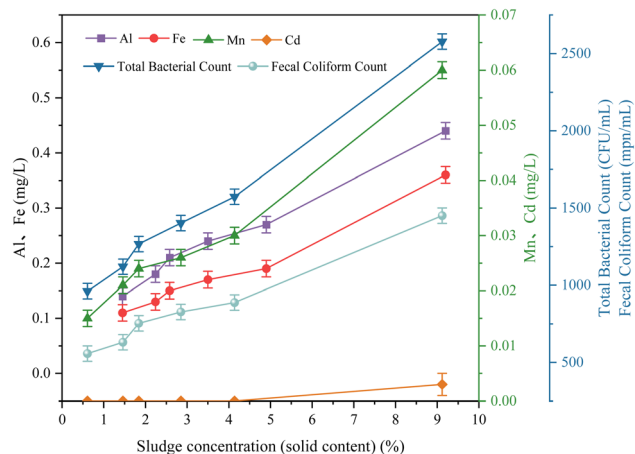


Fig. 12 Effect of discharge water concentration on supernatant Al, Fe, Mn, Cd, total bacteria and fecal coliform counts.

content also increased with an increase in the concentration, where a low concentration was without the reuse risk, a high concentration of microbial content exceeded the potential risk, but the metal content of Al, Fe, *etc.* was lower than water plant effluent, and the heavy metal content satisfied the drinking water standards.

In terms of coagulant dosage, when the concentration of discharged mud water was less than 4.14%, the supernatant after intensive coagulation treatment was of good quality; when the concentration reached 9.12%, the turbidity of the effluent did not meet the standard and some of the indexes exceeded the quality of the first water plant. To efficiently treat the actual concentration of mud water and high concentration of mud water during the abundant water period of the water purification plant, and to ensure the safety of its effluent water quality, in this test, different dosages of PFS-PDMDAAC were used to treat the mud water with 9.12% solid content, and the minimum dosage was  $13.65 \text{ mg L}^{-1}$ , the maximum dosage was set at  $31.5 \text{ mg L}^{-1}$ , the hydraulic parameters were unchanged, and the effluent indexes were measured after 30 min of static settling. In the determination of the effluent indicators, the test indicators are shown in Appendix Fig. S2,<sup>†</sup> and the indicators are shown in Fig. 13 and 14.

When the dosage was increased to  $15.75 \text{ mg L}^{-1}$ , the turbidity and most of the indicators of the effluent reached the water quality of a water plant, and some of the metals reached the drinking water standard; when the dosage was  $21 \text{ mg L}^{-1}$ , the turbidity was further reduced and some of the indicators reached the drinking water standard. When the dosage was increased, the turbidity decreased slightly, and the color, organic matter and metal iron content increased. In the case of turbidity and chromaticity, an increase in dosage caused them to decrease, while an overdosage caused the chromaticity to increase due to iron ions. The COD<sub>Mn</sub> content firstly decreased, and then increased, the  $\text{NH}_3\text{-N}$  and TP content gradually decreased, and a dosage of more than  $17.85 \text{ mg L}^{-1}$  caused the organic content of the supernatant to increase due to the increase in residual organic coagulant. In the case of metals, an

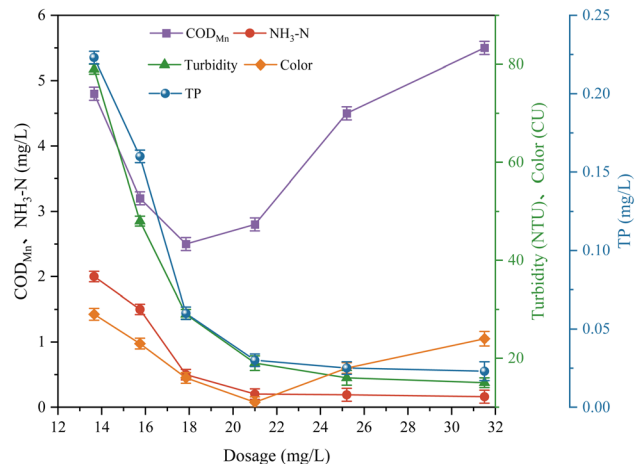


Fig. 13 Effect of coagulant dosage on COD<sub>Mn</sub>,  $\text{NH}_3\text{-N}$ , TP, turbidity and color of supernatant solution.

increase in dosage caused most of the metal content to decrease, where metal Fe decreased first, and then increased, and a dosage of more than  $17.85 \text{ mg L}^{-1}$  caused the metal Fe content to exceed the standard due to the increase in residual iron ions.

As shown in Fig. 14, when the coagulant dosage increased from  $13.65 \text{ mg L}^{-1}$  to  $21 \text{ mg L}^{-1}$ , the total bacterial count and fecal coliform count in the coagulated effluent decreased sharply, dropping from  $2980 \text{ CFU mL}^{-1}$  and  $1330 \text{ mpn per mL}$  to  $950 \text{ CFU mL}^{-1}$  and  $495 \text{ mpn per mL}$ , respectively, meeting the effluent water quality standards of the first water treatment plant. When the coagulant dosage further increased from  $21 \text{ mg L}^{-1}$  to  $31.5 \text{ mg L}^{-1}$ , the decline in total bacterial count and fecal coliform count slowed significantly, eventually reaching only  $790 \text{ CFU mL}^{-1}$  and  $340 \text{ mpn per mL}$ , respectively. This indicates that as the coagulant dosage increases, more microorganisms are destabilized along with colloidal particles and settle into the bottom sludge. At a dosage of  $21 \text{ mg L}^{-1}$ , PFS-PDMDAAC achieved the highest removal efficiency for

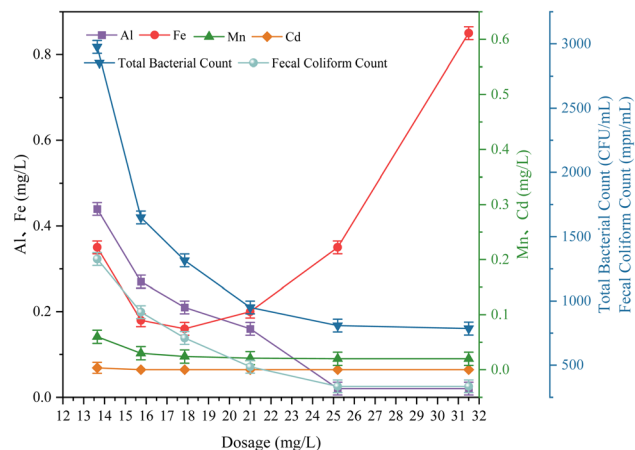


Fig. 14 Effect of coagulant dosage on supernatant Al, Fe, Mn, Cd, total bacterial counts and fecal coliform counts.

colloidal particles and microorganisms in the water, and further increasing the dosage provided marginal benefits. Therefore, from an economic perspective, the dosage should not exceed  $21 \text{ mg L}^{-1}$ .

### 3.4 Exploring the preliminary mechanism of intensive coagulation treatment of mud drainage water

To investigate the coagulation mechanism of high turbidity and high sediment discharge water from the Yellow River and verify the experimental effect of enhanced coagulation, the zeta potential of the supernatant and the morphology and particle size of the sludge flocs after enhanced coagulation were measured and analyzed with the discharge water with 2.5% solids as the object of the study.

**3.4.1 Zeta potential analysis.** Research shows that the coagulation effect and coagulation mechanism can be judged based on the zeta potential. In the one-factor test with different mixing ratios and dosages of the compound coagulant PFS-PDMAAC, the zeta potential was measured for the supernatant after coagulation and sedimentation of the discharged sludge to investigate the mechanism of enhanced coagulation and to verify its effect. The test results are shown in Fig. 15 and 16.

The zeta potential of the raw drainage water was measured to be  $-16.1 \text{ mV}$ , and thus the colloidal particles were negatively charged. When different mixing ratios of PFS-PDMAAC were added, the potential first changed from negative to positive with an increase in the mixing ratio, and then decreased to negative after reaching  $35 \text{ mV}$ . Employing the compound ratio of 1:15, the potential increased and the supernatant turbidity was  $399.5 \text{ NTU}$ , resulting in poor coagulation. This is due to the presence of more PDMDAAC, the positive charge and colloidal negative charge after neutralization made the sludge positively charged, resulting in the rejection of the absolute potential energy value and potential to become larger, colloidal stabilization, and weak adsorption bridging effect. At the compound ratio of 6:1, the

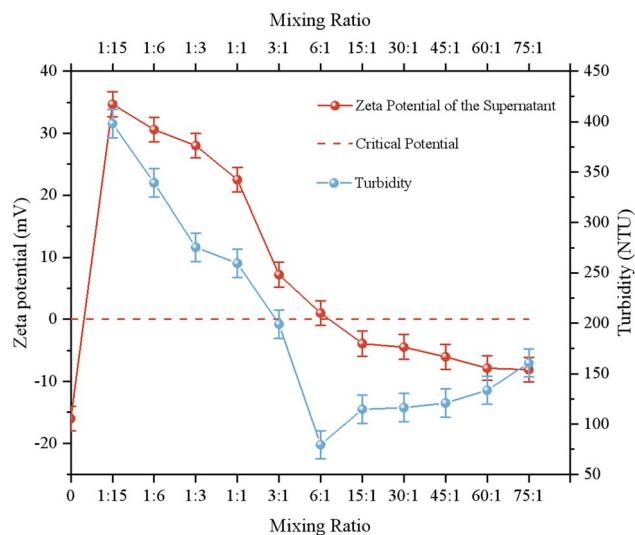


Fig. 15 Zeta potential of supernatant after adding different mixing ratios of coagulants.

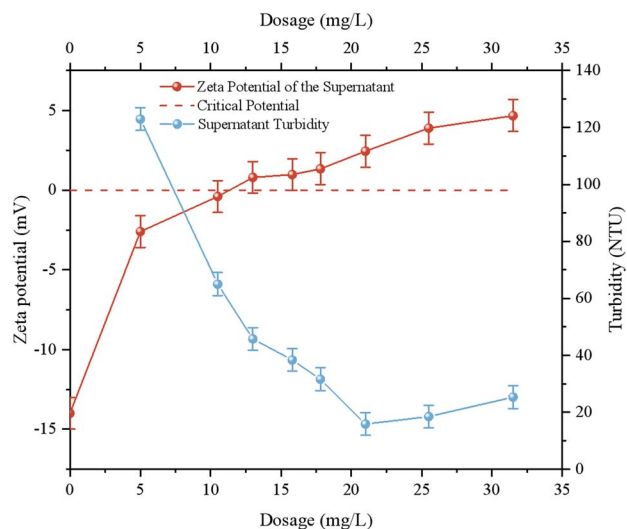


Fig. 16 Zeta potential of supernatant after treatment with different dosages of the coagulant.

potential declined, the turbidity was low as  $79.6 \text{ NTU}$ , and the coagulation was the best. This is because of the hydrolysis of positive charge and good colloidal negative neutralization, making the system unstable, the colloid easy to settle, and the compound ratio of coagulant exhibiting both an electrical neutralization and adsorption bridging effect, with first cohesion, and then bridging into a large floc. When the compound ratio increased from 6:1 to 75:1, the potential decreased, the turbidity increased, and the coagulation became worse because the cationic hydrolyzed polymer decreased, the electrical neutralization was weak, and the phenomenon of re-stabilization appeared. When the overall compound ratio was higher, the coagulation effect was good, and thus 6:1 was the best, mainly playing the role of adsorption bridging and electrical neutralization.

The original zeta potential of the drainage water was  $-14.1 \text{ mV}$ , and the colloids were stably suspended. With an increase in the coagulant dosage, the potential increased gradually from  $-14.1 \text{ mV}$ , and the absolute value first decreased, and then increased. When the dosage reached  $10.5 \text{ mg L}^{-1}$ , the potential was close to the critical potential, and the turbidity decreased, but it was not the best dosage, which indicated that the destabilizing and coagulating effect may not be the best when the potential is close to the critical level. When the dosage increased from  $10.5 \text{ mg L}^{-1}$  to  $21 \text{ mg L}^{-1}$ , the potential increase was small, but the turbidity decreased greatly because the coagulant, in addition to electrical neutralization, caused the polymer chain adsorption and bridging effect to be strong, and the colloid formation of floc settlement and the iron hydroxide precipitation had a neutralization and net paving sweeping effect. When the dosage increased from  $21 \text{ mg L}^{-1}$  to  $31.5 \text{ mg L}^{-1}$ , the potential increased, the turbidity increased because of the overdosage, the polymer chain produced colloid protection, and the phenomenon of re-stabilization occurred. Therefore, the dosage of  $21 \text{ mg L}^{-1}$  is the best for turbidity



removal, which mainly plays the role of adsorption and bridging, and also has the role of electrical neutralization and net paving and sweeping.

**3.4.2 Analysis of floc morphology.** To more comprehensively observe the flocculation changes in the discharged mud water after enhanced coagulation and analyze the enhanced coagulation effect from macro and microscopic perspectives,<sup>31</sup> the surface morphology of the sludge flocs after enhanced coagulation of the discharged mud water was photographed and observed by combining the actual observation of the sedimentation effect and scanning electron microscopy,<sup>32</sup> and the results are shown in Figs. S3 and S4.†

In Figs. S3 and S4,† it can be seen that the size, morphology and structure of the sludge flocs after intensive coagulation treatment of drainage water were completely different from that when the drainage water was untreated. In Fig. S3,† it can be seen that in (a) there are almost no floc-like particles, but a large number of fine suspended particles pooled together, with almost no pores, belonging to poor settlement and (b) the figure is almost all floc particles, and the floc obviously became coarser, and the pores between the floc particles also increased, and the settlement was better. In Fig. S4,† it can be seen that the particle volume in (a) is smaller and the structure is tight, the surface is more regular and strict, the porosity is small, and its dewatering performance is poor and in (b) the floc volume and particle size increased, which is more favorable for settlement, and the porosity is larger and the structure is loose and porous, causing the dewatering performance to be better.

**3.4.3 Analysis of sludge floc particle size.** The enhanced coagulation effect of sludge water is affected by many factors, among which the coagulant dosage and floc particle size are the key factors.<sup>33</sup> Research shows that the larger the floc particle size, the better the settling performance, the smaller the specific resistance, and the better the dewatering. Employing a laser particle size analyzer, it was found that the average particle size of the drainage water was 38.3  $\mu\text{m}$ , and 90% of the floc particle size was less than 54.6  $\mu\text{m}$ , which had a poor natural sedimentation performance. After the addition of PFS-PDMDAAC, the particle size of the sludge particles increased significantly, and the settling performance was improved. In the rapid mixing stage, the coagulant was mixed with the sludge discharge water rapidly, and the colloidal particles were destabilized and coalesced to form larger flocs, but the floc density was low; in the slow flocculation stage, the flocs formed larger and denser particles through bridging, which further improved the settling performance.

The experimental results showed that with an increase in the PFS-PDMDAAC dosage, the particle size distribution of the sludge flocs showed a trend of increasing, and then decreasing. When the dosage was 5.25  $\text{mg L}^{-1}$ , the average floc particle size increased to 84  $\mu\text{m}$  ( $D_{50} = 91.1 \mu\text{m}$ ,  $D_{90} = 152 \mu\text{m}$ ), which was 2.19 times of that of the discharged sludge water, and the settling performance was significantly improved; when the dosage was 21  $\text{mg L}^{-1}$ , the floc particle size reached the maximum, and the average particle size was 238  $\mu\text{m}$  ( $D_{50} = 244 \mu\text{m}$ ,  $D_{90} = 328 \mu\text{m}$ ), which was 6.21 times of that of the discharged sludge water. At this time, the settling performance was

optimal, and the turbidity and  $\text{SV}_{30}$  of the supernatant were 15.7 NTU and 18.2%, respectively. However, when the dosage was increased to 31.5  $\text{mg L}^{-1}$ , the floc particle size decreased to 101  $\mu\text{m}$  ( $D_{50} = 107 \mu\text{m}$ ,  $D_{90} = 173 \mu\text{m}$ ), and the turbidity and  $\text{SV}_{30}$  of the supernatant increased to 25.3 NTU and 19.1%, respectively, and the sedimentation performance was weakened, which was probably due to the protective effect of the colloid. In conclusion, the enhanced coagulation effect of the discharged mud water was positively correlated with the floc particle size, and the moderate dosage of coagulant could significantly improve the settling performance, but an excessive dosage would weaken the coagulation effect.

## IV Conclusion

(1) It was shown that under the conditions of a fixed concentration of influent water, factors such as coagulant type, compounding ratio, dosage, hydraulic conditions and water temperature had a significant effect on the treatment effect of drainage water. The optimization experiments showed that the best treatment effect was achieved with the PFS-PDMDAAC compound coagulant (6 : 1 ratio), dosage of 13.65  $\text{mg L}^{-1}$ , rapid agitation (300 rpm, 1.5 min) combined with slow agitation (120 rpm, 7 min), and a water temperature of 20  $^{\circ}\text{C}$ , which reduced the turbidity of the supernatant to 46.2 NTU and the specific resistance of the sludge to less than  $0.94 \times 10^{12} \text{ m kg}^{-1}$ , and the solid content was more than 8%, which meets the requirement of direct dewatering. Its mechanism of action is PFS compresses the bilayer to reduce the zeta potential through electric neutralization, while PDMDAAC promotes the growth of flocs through adsorption and bridging and net catching sweeping, and the best synergistic effect was achieved by the 6 : 1 compound ratio; the dosage of 13.65  $\text{mg L}^{-1}$  ensured that the colloids were fully destabilized and at the same time, avoided the phenomenon of re-stabilization caused by the reversal of the electric charge; the optimized hydraulic conditions not only guaranteed the uniform dispersion of the coagulant, but also promoted the effective aggregation of flocs; and the water temperature of 20  $^{\circ}\text{C}$  maintained the activity of the coagulant and the rate of molecular movement, which guaranteed the overall coagulation efficiency.

(2) This study showed that the concentration of the discharged sludge water had a significant effect on the enhanced coagulation effect, which was characterized by concentration dependence. When treating a low concentration of discharged sludge water (<4.14%), a coagulant dosage of 13.65  $\text{mg L}^{-1}$  achieved a good treatment effect, which is mainly due to the large spacing of colloidal particles, and this the coagulant could fully cover the particle surface and achieve a high efficiency of destabilization and flocculation; in the mid-concentration range (4.14–9.12%), it was necessary to increase the dosage to 21  $\text{mg L}^{-1}$  to maintain the treatment effect, which is due to the increased collision probability of particles caused by the increase in colloidal concentration, where more coagulant was needed to maintain the balance of electro-neutralization and adsorption and bridging. When the concentration exceeded 9.12%, even if the dosage increased, the treatment effect was



still difficult to reach the effluent standard, indicating that there is an obvious upper concentration limit in the application of enhanced coagulation technology. The mechanism mainly involves two aspects, where on the one hand, the spacing of colloidal particles decreases under high concentration conditions, leading to electrostatic repulsion and increase in the spatial resistance effect, making it difficult for the coagulant to effectively cover all the particles, which affects the formation of flocs; on the other hand, the excessive addition of the coagulant may trigger the phenomenon of charge inversion (zeta potential changes from negative to positive), which results in colloidal re-stabilization, and at the same time, excess coagulant may form a colloidal protective layer, which inhibits the further aggregation of the flocs, and ultimately leads to a decline in the sedimentation performance. Thus, the results of this study are of great significance in optimizing the coagulation treatment process for different concentrations of drainage water.

(3) Through the systematic analysis of zeta potential, floc morphology and particle size, the mechanism of enhanced coagulation was revealed in depth. The zeta potential analysis showed that the absolute potential value was the smallest (close to 0) under the conditions of compound ratio of 6:1, at this time, the  $\text{Fe}^{3+}/\text{Fe}(\text{OH})_3$  provided by PFS effectively neutralized the negative charge on the surface of the colloid, and the synergistic effect with PDMDAAC caused the colloidal particles to reach the optimal destabilization state, and at this time, van der Waals force dominated and significantly promoted the collision bonding between the particles. The observation of floc morphology showed that the floc formed by enhanced coagulation had a significantly increased volume and loose porous structure, and this special morphology not only improved the settling rate by enhancing the gravity settling effect, but also reduced the content of bound water due to its porous characteristics, which significantly improved the performance of sludge dewatering. The particle size analysis further confirmed that the average floc particle size increased from  $38.3\text{ }\mu\text{m}$  to  $238\text{ }\mu\text{m}$  at the optimal dosage of  $21\text{ mg L}^{-1}$ , which was due to the synergistic effect of the electrical neutralization and adsorption bridging by the coagulant; however, when the dosage was higher than  $21\text{ mg L}^{-1}$ , the spatial resistance effect and possible charge reversal of the coagulant led to a decrease in the floc particle size and colloid re-stabilization, which ultimately affected the sedimentation performance.

## Data availability

The experimental data used in this study were first published on the web and are free of plagiarism. Additionally, all relevant data used in this study are available from the corresponding author.

## Author contributions

The concept and design of the study were collaborative efforts among all the authors. Hairong Yan was in charge of data collection, material preparation, and analysis. Xiaosan Song, Qingchao Shen, Wenjing Sun, Ping Li and Wenxuan Wei wrote

the first draft of the paper, and subsequent drafts were revised with insight from all the authors. The final draft of this paper was reviewed and approved by all the authors.

## Conflicts of interest

No conflict of interest was reported by the authors.

## Acknowledgements

This study was supported by the Research Program for Gansu Provincial Science and Technology Program (20JR10RA228).

## References

- 1 J. Chen, F. Wang and D. He, Geochemistry of water quality in the Yellow River, *Earth Science Frontiers*, 2006, (01), 58–73.
- 2 Y. Ding, X. Li, D. Wang, J. Xu and Y. Yu, Study on Spatial and Temporal Differences of Water Resource Sustainable Development and Its Influencing Factors in the Yellow River Basin, China, *Sustainability*, 2023, **15**(19), 14316.
- 3 J. Qin, Y.-J. Ding, Q.-D. Zhao, S.-P. Wang and Y.-P. Chang, Assessments on surface water resources and their vulnerability and adaptability in China, *Adv. Clim. Change Res.*, 2020, **11**, 381–391.
- 4 H. A. Faber, K. C. Klomp, *et al.*, AWWA Research Foundation Report: Disposal of Wastes from Water Treatment Plants – Part 4, *J. - Am. Water Works Assoc.*, 1970, **62**(1), 63–70.
- 5 C. Lai and S. Lin, Treatment of chemical mechanical polishing wastewater by electrocoagulation: system performances and sludge settling characteristics, *Chemosphere*, 2004, **54**(3), 235–242.
- 6 Y. Hsueh, F. Wu, Q. Ye, S. Lai and Y. Tsang, Reservoir Mud Releasing May Suboptimize Fluvial Sand Supply to Coastal Sediment Budget: Modeling the Impact of Shihmen Reservoir Case on Tamsui River Estuary, *Water Resour. Res.*, 2024, **60**(6), e2023WR036701.
- 7 S. Liu, Q. Shao, J. Ning, L. Niu, X. Zhang, G. Liu and H. Huang, Remote-Sensing-Based Assessment of the Ecological Restoration Degree and Restoration Potential of Ecosystems in the Upper Yellow River over the Past 20 Years, *Remote Sens.*, 2022, **14**, 3550.
- 8 B. Cui, Q. Yang, Z. Yang and K. Zhang, Evaluating the ecological performance of wetland restoration in the Yellow River Delta, China, *Ecol. Eng.*, 2009, **35**, 1090–1103.
- 9 B. Bień and J. D. Bień, Conditioning of Sewage Sludge with Physical, Chemical and Dual Methods to Improve Sewage Sludge Dewatering, *Energies*, 2021, **14**, 5079.
- 10 T. Ahmad, K. Ahmad, A. Ahad and M. Alam, Characterization of water treatment sludge and its reuse as coagulant, *J. Environ. Manage.*, 2016, **182**, 606–611.
- 11 J. Azadi, K. Yamauchi, K. Matsubara and N. Katagiri, Enhancement in Dewatering Efficiency of Disrupted Sludge through Ultrasonication and Re-Flocculation—Sustainable Sludge Management, *Sustainability*, 2024, **16**, 7427.
- 12 Q. Guan, H. Zheng, M. Tan, X. Tang, X. Zheng, Y. Liao and W. Fan, Advances on Sludge Properties and Dewaterability

- with Chemical Conditioning: A Review, *Asian J. Chem.*, 2014, **26**(8), 2199–2203.
- 13 K. Meaghan, Gibbons. Understanding removal of phosphate or arsenate onto water treatment residual solids, *J. Hazard. Mater.*, 2011, **186**(2–3), 1916–1923.
- 14 J. K. Edzwald and J. E. Tobiason, Enhanced coagulation: US requirements and a broader view, *Water Sci. Technol.*, 1999, **40**(9), 63–70.
- 15 D. Wang, H. Liu, M. Yan, *et al.*, Enhanced coagulation and optimized coagulation: necessity, research progress and development direction, *J. Environ. Sci.*, 2006, (04), 544–551.
- 16 O. M. Olukowi, Y. Xie, Z. Zhou, I. O. Adebayo and Y. Zhang, Performance improvement and mechanism of composite PAC/PDMDAAC coagulant via enhanced coagulation coupled with rapid sand filtration in the treatment of micro-polluted surface water, *J. Environ. Chem. Eng.*, 2022, **10**(5), 108450.
- 17 M. Yan, K. Guo, Y. Gao, Q. Yue and B. Gao, Insights into the control mechanism of different coagulation pretreatment on ultrafiltration membrane fouling for oily wastewater treatment, *Sep. Purif. Technol.*, 2023, **327**, 124907.
- 18 J. Hou, C. Hong, W. Ling, J. Hu, W. Feng, Y. Xing, Y. Wang, C. Zhao and L. Feng, Research progress in improving sludge dewaterability: sludge characteristics, chemical conditioning and influencing factors, *J. Environ. Manage.*, 2024, **351**, 119863.
- 19 R. Li, Y. Zhang, J. Tang, *et al.*, Research on high performance polyaluminum chloride, *Chin. Water Supply Drainage*, 2010, **26**(23), 73–75.
- 20 Y. Xu, W. Sun, D. Wang, *et al.*, Coagulation of micro-polluted Pearl River water with IPF-PACls, *J. Environ. Sci.*, 2004, **16**(4), 585–588.
- 21 A. I. Zouboulis, P. A. Moussas and F. Vasilakou, Polyferric sulphate: preparation, characterisation and application in coagulation experiments, *J. Hazard Mater.*, 2008, **155**(3), 459–468.
- 22 M. F. S. Gisi, O. Navratil, F. Cherqui, *et al.*, From dishwasher to river: how to adapt a low-cost turbidimeter for water quality monitoring, *Environ. Monit. Assess.*, 2024, **196**, 1180.
- 23 M. R. Karim, M. M. M. Syeed, A. Rahman, *et al.*, A Comprehensive Dataset of Surface Water Quality Spanning 1940-2023 for Empirical and ML Adopted Research, *Sci. Data*, 2025, **12**, 391.
- 24 S. Yaman, N. Karasekreter and U. Ergün, Determination of free chlorine concentration and pH of the water using neural network based colorimetric method, *Chem. Pap.*, 2022, **76**, 5721–5732.
- 25 P. Wang, Y. Tian, C. Liu, *et al.*, Development and application of a miniature rapid detection device for ammonia nitrogen in environmental waters, *Anal. Chem.*, 2024, **52**(02), 178–189, DOI: [10.19756/j.issn.0253-3820.231287](https://doi.org/10.19756/j.issn.0253-3820.231287).
- 26 Y. Nakaya, J. Jia and H. Satoh, Tracing morphological characteristics of activated sludge flocs by using a digital microscope and their effects on sludge dewatering and settling, *Environ. Technol.*, 2023, **45**(20), 4042–4052.
- 27 C. Campos-Pinilla, M. Cárdenas-Guzmán and A. Guerrero-Cañizares, Behavior of the indicators of faecal contamination in different types of waters of the Bogotá savanna (Colombia), *Univ. Sci.*, 2008, **13**(2), 103–108.
- 28 H. Yin, A. Truskewycz and I. S. Cole, Quantum dot (QD)-based probes for multiplexed determination of heavy metal ions, *Microchim. Acta*, 2020, **187**, 336.
- 29 A. A. Ramlee, A. M. Som, S. W. Puasa, *et al.*, Coagulation–flocculation mechanism and characterisation of *Hylocereus undatus* foliage as a natural coagulant in industrial wastewater treatment, *Chem. Pap.*, 2023, **77**, 6083–6093.
- 30 J. Wang, Y. Wang, T. Ma, G. Xu and M. Feng, Synergistic mechanism of adsorption-diffusion at quartz-water interface for the dewatering of waste slurry using APAM flocculant: Insights from molecular dynamics simulation, *J. Water Proc. Eng.*, 2023, **55**, 104275.
- 31 Y. Kong, Y. Zhou, P. Zhang, Y. Nie and J. Ma, Coagulation performance and mechanism of different novel covalently bonded organic silicon-aluminum/iron composite coagulant for As(V) removal from water: the role of hydrolysate species and the effect of coexisting microplastics, *J. Hazard. Mater.*, 2024, **480**, 135819.
- 32 D. I. Verrelli, D. R. Dixon and P. J. Scales, Assessing dewatering performance of drinking water treatment sludges, *Water Res.*, 2010, **44**(5), 1542–1552.
- 33 W. Yin, Y. Xie and Z. Zhu, Literature overview of basic characteristics and flotation laws of flocs, *Int. J. Miner. Metall. Mater.*, 2024, **31**, 943–958.